IRF2BPL Is Associated with Neurological Phenotypes

Paul C. Marcogliese,[1,25] Vandana Shashi,[2,25] Rebecca C. Spillmann,[2] Nicholas Stong,[3] Jill A. Rosenfeld,[1] Mary Kay Koenig,[4] Julián A. Martínez-Agosto,[5,6,7] Matthew Herzog,[5] Agnes H. Chen,[8] Patricia I. Dickson,[8] Henry J. Lin,[8] Moin U. Vera,[8] Noriko Salamon,[9] Damara Ortiz,[10] Elena Infante,[10] Wouter Steyaert,[11] Bart Dermaut,[11] Bruce Poppe,[11] Hyung-Lok Chung,[1] Zhongyuan Zuo,[1] Pei-Tseng Lee,[1] Oguz Kanca,[1] Fan Xia,[1] Yaping Yang,[1] Edward C. Smith,[12] Joan Jasien,[12] Sujay Kansagra,[12] Gail Spiridigliozzi,[13] Mays El-Dairi,[14] Robert Lark,[15] Kacie Riley,[2] Dwight D. Koeberl,[2] Katie Golden-Grant,[16] Program for Undiagnosed Diseases (UD-PrOZA), Undiagnosed Diseases Network, Shinya Yamamoto,[1,17,18,19] Michael F. Wangler,[1,17,18] Ghayda Mirzaa,[20,21] Dimitri Hemelsoet,[22] Brendan Lee,[1] Stanley F. Nelson,[5] David B. Goldstein,[3] Hugo J. Bellen,[1,17,18,19,23,*] and Loren D.M. Pena[2,24,*]

Interferon regulatory factor 2 binding protein-like (*IRF2BPL*) encodes a member of the IRF2BP family of transcriptional regulators. Currently the biological function of this gene is obscure, and the gene has not been associated with a Mendelian disease. Here we describe seven individuals who carry damaging heterozygous variants in *IRF2BPL* and are affected with neurological symptoms. Five individuals who carry *IRF2BPL* nonsense variants resulting in a premature stop codon display severe neurodevelopmental regression, hypotonia, progressive ataxia, seizures, and a lack of coordination. Two additional individuals, both with missense variants, display global developmental delay and seizures and a relatively milder phenotype than those with nonsense alleles. The *IRF2BPL* bioinformatics signature based on population genomics is consistent with a gene that is intolerant to variation. We show that the fruit-fly *IRF2BPL* ortholog, called *pits* (protein interacting with Ttk69 and Sin3A), is broadly detected, including in the nervous system. Complete loss of *pits* is lethal early in development, whereas partial knockdown with RNA interference in neurons leads to neurodegeneration, revealing a requirement for this gene in proper neuronal function and maintenance. The identified *IRF2BPL* nonsense variants behave as severe loss-of-function alleles in this model organism, and ectopic expression of the missense variants leads to a range of phenotypes. Taken together, our results show that *IRF2BPL* and *pits* are required in the nervous system in humans and flies, and their loss leads to a range of neurological phenotypes in both species.

Introduction

The etiology of neurodevelopmental disorders can vary and can include prenatal exposures, maternal disease, multifactorial causes, and single genes. *De novo* genomic contributions were recently highlighted in a large cohort studied as part of the Deciphering Developmental Disorders Study, wherein an estimated 42% of the cohort carried pathogenic *de novo* mutations in the coding region of genes.[1–3] The phenotypic and genomic heterogeneity of neurodevelopmental disorders can pose a diagnostic challenge. Several known Mendelian disorders, such as Rett syndrome (MIM: 312750), the neuronal ceroid lipofuscinoses (NCLs), and X-linked adrenoleukodystrophy (X-ALD [MIM: 300100]) display neurodevelopmental regression as a common element and illustrate the range of symptoms and pathologies associated with neurological symptoms. The known or proposed mechanisms of disease can include altered transcriptional control (Rett syndrome),[4,5] accumulation of a substrate with loss of neurons (juvenile infantile NCL [MIM: 204200]),[6,7] or inflammation and demyelination (X-ALD).[8–10] More recently, new associations of genes

[1]Department of Molecular and Human Genetics, Baylor College of Medicine, Houston, TX 77030, USA; [2]Division of Medical Genetics, Department of Pediatrics, Duke University School of Medicine, Durham, NC 27710, USA; [3]Institute for Genomic Medicine, Columbia University Medical Center, New York, NY 10032, USA; [4]Division of Child & Adolescent Neurology, Department of Pediatrics, The University of Texas Health Science Center at Houston, Houston, TX 77030, USA; [5]Department of Human Genetics, David Geffen School of Medicine, University of California, Los Angeles, Los Angeles, CA 90095, USA; [6]Department of Pediatrics, David Geffen School of Medicine, University of California, Los Angeles, Los Angeles, CA 90095, USA; [7]Department of Child and Adolescent Psychiatry, Resnick Neuropsychiatric Hospital, University of California, Los Angeles, Los Angeles, CA 90095, USA; [8]Department of Pediatrics, Los Angeles Biomedical Research Institute at Harbor-UCLA Medical Center, Torrance, CA 90502, USA; [9]Department of Radiology, David Geffen School of Medicine, University of California, Los Angeles, Los Angeles, CA 90095, USA; [10]Children's Hospital of Pittsburgh, University of Pittsburgh Medical Center, University of Pittsburgh, Pittsburgh, PA 15224, USA; [11]Department of Medical Genetics, Ghent University Hospital, 9000 Ghent, Belgium; [12]Division of Neurology, Department of Pediatrics, Duke University School of Medicine, Durham, NC 27710, USA; [13]Department of Psychiatry and Behavioral Sciences, Duke University School of Medicine, Durham, NC 27710, USA; [14]Department of Ophthalmology, Duke University School of Medicine, Durham, NC 27710, USA; [15]Department of Orthopedic Surgery, Duke University School of Medicine, Durham, NC 27710, USA; [16]Division of Genetic Medicine, Seattle Children's Hospital, Seattle, WA 98105, USA; [17]Program in Developmental Biology, Baylor College of Medicine, Houston, TX 77030, USA; [18]Jan and Dan Duncan Neurological Research Institute, Texas Children's Hospital, Houston, TX 77030, USA; [19]Department of Neuroscience, Baylor College of Medicine, Houston, TX 77030, USA; [20]Center for Integrative Brain Research, Seattle Children's Research Institute, Seattle, WA 98105, USA; [21]Department of Pediatrics, University of Washington, Seattle, WA 98105, USA; [22]Department of Neurology, Ghent University Hospital, 9000 Ghent, Belgium; [23]Howard Hughes Medical Institute, Baylor College of Medicine, Houston, TX 77030, USA
[24]Present address: Cincinnati Children's Hospital, Cincinnati, OH 45229, USA
[25]These authors contributed equally to this work
*Correspondence: hbellen@bcm.edu (H.J.B.), loren.pena@cchmc.org (L.D.M.P.)
https://doi.org/10.1016/j.ajhg.2018.07.006.

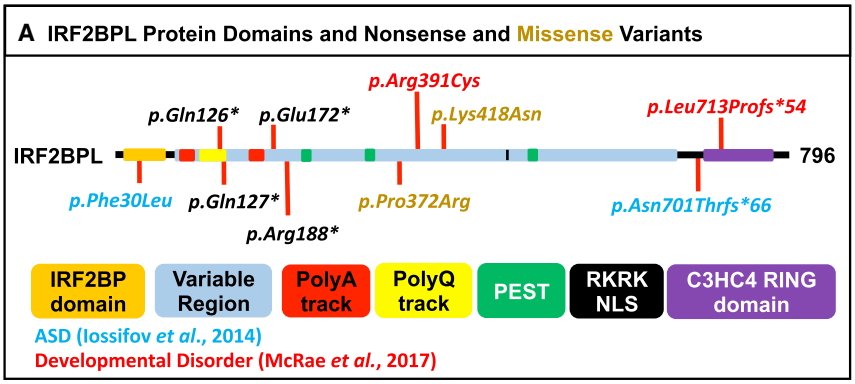

B IRF2BPL tolerance to change and predicted inheritance

Probability of LoF intolerance (pLI)			Missense Constraint			DOMINO	
Expected	Observed	pLI score	Expected	Observed	z score	Score	Inheritance prediction
10.5	0	0.97	384.8	195	4.73	0.962	Very likely dominant

Figure 1. IRF2BPL Protein Structure and Gene Constraint

(A) IRF2BPL is 796 amino acids (aa) long and contains two highly conserved domains (IRF2BP zinc finger and C3HC4 RING finger) at the N and C termini. Within the variable region are multiple polyalanine and PEST sequences and a 25 aa polyglutamine tract (amino acids 103–127). All four nonsense variants occur early in the transcript before the predicted PEST sequences, and the two missense variants (highlighted in gold) occur in the middle of the protein. We included *de novo* variants discovered in large-scale sequencing studies for autism spectrum disorders (ASD, highlighted in blue) and developmental disorders (highlighted in red).

(B) *IRF2BPL* is highly constrained on the basis of the lack of LoF variants in ExAC,[20] resulting in a high probability-of-LoF-intolerance (pLI) score and missense constraint *Z* score. Predictions based on the DOMINO algorithm indicate that variation in IRF2BPL is likely to lead to a dominantly inherited disease.

with severe developmental phenotypes and neurodegeneration have been discovered.[11,12] This has been largely possible as a result of high-throughput sequencing methods such as next-generation sequencing (NGS), in conjunction with sequencing databases for control cohorts such as ExAC and gnomAD,[13–21] variant prediction,[22] model organism information (e.g., MARRVEL)[23] and crowdsourcing programs, such as GeneMatcher,[24] used for identifying additional cases. These tools have greatly promoted gene discovery and assisted in ascertaining the role of the candidate variants for disease. Programs such as the Undiagnosed Diseases Network (UDN)[25,26] promote multi-site collaboration that combines NGS and functional data that facilitate the diagnosis of rare disorders.

Here we describe a cohort of seven individuals, ascertained for neurological symptoms, who share predicted pathogenic variants in *IRF2BPL* (MIM: 611720), an intronless gene at 14q24.23.[27] The transcript is expressed in many organs, including in central nervous system (CNS) components such as the cerebellum (GTex, accessed January 29, 2018; see Web Resources).[28] IRF2BPL and its two mammalian paralogs, IRF2BP1 and IRF2BP2, share two highly conserved domains. These include a coiled-coil DNA binding domain (IRF2BP zinc finger domain) at the amino terminus and a C3HC4-type RING finger domain at the carboxyl terminus. IRF2BPL also contains polyglutamine and polyalanine tracts. In between the two conserved domains is a variable region that contains a potential nuclear targeting signal.[27] IRF2BPL also contains several putative PEST (proline, glutamic acid, serine, and threonine-rich) sequences, suggesting that this protein is post-translationally regulated[29] (Figure 1A).

IRF2BPL has been proposed to have a role in the initiation of puberty in female non-human primates and rodents.[30] It acts as a transcriptional activator for gonadotropin-releasing hormone in the CNS.[30] Expression of *Irf2bpl* in the hypothalamus of female rats increases during puberty, and site-specific reduction of *Irf2bpl* in the preoptic area disrupts the estrus cycle.[31] In addition, IRF2BPL has also recently been proposed to function as an E3 ubiquitin ligase that targets β-catenin for proteasome degradation in gastric cancer.[32] Despite these studies, the *in vivo* function of IRF2BPL in all species remains largely undefined. Here we describe a role for *IRF2BPL* in the functional and structural maintenance of the nervous system. We provide evidence in seven individuals and use functional assays in fruit flies to support the findings that these variants cause dramatic changes to IRF2BPL function and that IRF2BPL plays a role in both development and neuronal maintenance.

Subjects and Methods

Oversight for the human subjects research protections was provided by the institutional review board (IRB) of the National Human Genome Research Institute (protocol 15-HG-0130, Clinical and Genetic Evaluation of Patients with Undiagnosed Disorders through the Undiagnosed Diseases Network) and the Duke University School of Medicine IRB (Pro00056651).

Demographics, Ascertainment, and Diagnoses

The individuals are all unrelated and between 2.5 and 43 years of age; this includes one person who died at 15 years of age. Four are male, six are of European descent, and one was identified as Hispanic. They were evaluated by the genetics or neurology service as part of clinical care for neurological symptoms (subjects 2 and 4–7) or as participants (subjects 1 and 3) in the UDN.[26] In non-UDN cases, use of the GeneMatcher website[24] facilitated ascertainment of two of the subjects (6 and 7); the UDN page for *IRF2BPL*

Table 1. Salient Clinical Features for Each Subject

	Subject 1	Subject 2	Subject 3	Subject 4	Subject 5	Subject 6	Subject 7
IRF2BPL variant	c.584G>T (p.Gly195Val) and c.514G>T (p.Glu172*), complex rearrangement, Sanger confirmed, *de novo*	c.562C>T (p.Arg188*), Sanger confirmed, no parents available for testing	c.562C>T (p.Arg188*), Sanger confirmed, *de novo*	c. 379C>T (p.Gln127*), Sanger confirmed, no parents available for testing	c.376C>T (p. Gln126*), Sanger confirmed, *de novo*	c.1115C>G (p.Pro372Arg, Sanger confirmed, *de novo*	c.1254G>C (p.Lys418Asn), Sanger confirmed, *de novo*
Gender	male	female	male	female	male	male	female
Current age	7 years	deceased at 15 years	20 years	16 years	43 years	11 years	2.5 years
Growth for age at most recent visit (*Z* score)	6 years, 6 months: Wt 20.1 kg (−0.42), Ht 116.8 cm (−0.67), HC 51.4 cm (−0.17)	13 years: Wt 45 kg (0.5), Ht 168 cm (2)	20 years: Wt 66 kg (−0.43), Ht 141 cm (−5.0), HC 59 cm (2.4)	15 years: Wt 46.9 kg (−0.5), Ht 162.4 cm (0), HC 52 cm (−2)	NA	11 years, 2 months: Wt 32.6 kg (−0.62), Ht 125 cm (−2.81), HC 51 cm (−1.13)	2 years, 1 month: Wt 13.30 kg (0.5), Ht 86.30 cm (−1), HC 49.40 cm (1)
Developmental delays preceding regression	present	none	none	present	NA	present	none
Age of onset of motor regression	2.5–3 years	5–6 years	5–6 years	unknown	5–10 years	no regression	no regression
Current speech and language skills	no speech at 6.5 years of age	lack of speech since 11 years	lack of speech since 10 years	NA	NA	speech regression at 3.5 years and essentially non-verbal	no speech development
Current gross motor skills	wheelchair bound since 5.5 years	in a wheelchair since 9 years	non-ambulatory since 10 years	unsteady gait, clumsy, mostly wheelchair dependent	wheelchair bound since 28 years	normal stance and gait, tandem and reciprocal	walks easily up and down stairs, starting to run
Current oromotor skills	mild to moderate oropharyngeal dysphagia, silent aspiration and tube feeding	dysphagia at 10 years, requiring tube feeding	progressive dysphagia at 10 years, requiring tube feeding at 13 years	silent aspiration at 15 years with tube feeding	NA	normal	normal
Seizures	diagnosed with seizures at 6 years	staring spells	myoclonus at 10 years	seizures at 6 years	febrile, photosensitive, and myoclonic epilepsy at 10 years	generalized myoclonic epilepsy at 14 months	infantile spasms at 6 months
Movement abnormalities	ataxia, dystonia, choreoathetosis	dystonia, no ataxia	ataxic gait at 6 years	lower-extremity dystonia at 15 years	ataxia, choreoathetosis, generalized dystonia since 15 years of age	none	none
Other neurological findings	spasticity, cerebellar signs	NA	spasticity, cerebellar signs, positive Romberg signs, and bilateral Babinski signs by 7 years	NA	hyperreflexia	none	none

(*Continued on next page*)

Table 1. *Continued*

	Subject 1	Subject 2	Subject 3	Subject 4	Subject 5	Subject 6	Subject 7
EEG	abnormal at 5 years with diffuse slowing, interictal discharges from left occipital and right temporal lobes	mild background slowing at 9 and 13 years, normal at 9 and 14 years	normal at 13 years	abnormal since 6 years	abnormal since 10 years	abnormal with generalized spike and wave at 6 years	abnormal at 6 months
Brain MRI	normal at 5 years	"bulky" corpus callosum, mild cerebellar volume loss, large left middle cranial fossa arachnoid cyst at 8 years, marked cord thinning on spine MRI at 10 years	normal at 7 years, diffuse cerebral atrophy at 13 years, cerebral atrophy at 20 years	normal at 6 and 13 years	cerebral, cerebellar, brainstem, and corpus callosum atrophy at 34 years	probable Rathke's cyst at 11 years, otherwise normal	normal at 6 months and 2 years

Abbreviations are as follows: wt, weight; Ht, height; HC, head circumference; NA, not available; EEG, electroencephalography.

facilitated contact with subject 5, and subjects 2 and 4 were ascertained through communication with the clinical lab that performed whole-exome sequencing (WES). WES for subjects 1, 3, and 5–7 was performed in the proband plus the parents, and WES for subjects 2 and 4 was performed in the proband only. WES was performed with written informed consent for clinical sequencing and in accordance with guidelines from the institutional review board for research sequencing for all subjects. Consent for publication and images was obtained from all guardians.

The seven subjects reported here have a constellation of neurological findings of variable severity. Although almost all suffered from epilepsy (Human Phenotype Ontology[33] term [HP:0001250]), those with nonsense variants in *IRF2BPL* had severe, progressive neurodevelopmental regression (HP: 0002376), dysarthria (HP:0001260), spasticity (HP:0001257), and symptoms of movement disorders (HP:0100022). There was also cerebral and cerebellar volume loss in the two oldest subjects (3 and 5; HP:0002506 and HP:0007360). In contrast, the two subjects with missense variants have a generally milder course, with symptoms of epilepsy, speech delay (HP:0000750), and hypotonia (HP:0009062). Full clinical descriptions for each proband are in the Supplemental Note and in Table 1 and Table S1 as well as Video S1 and Video S2.

Methods

Exome Sequencing

Subjects had WES performed on a clinical or research basis. Exome data are summarized in Table S3. Across the performing labs, the minimum average depth of coverage was 100× across assays, and minimum proportion of the target at >10× coverage was 95%.

Exome Reanalysis for Subject 1

FASTQ files were obtained from the relevant source with parental consent. Alignment and variant calling were performed as previously described.[34] Novel genotypes were filtered for quality and observations in a control public database. We highlighted variants in known OMIM genes or mouse essential genes and loss-of-function (LoF) variants that are in genes with known pathogenic LoF variants, genes reported as haploinsufficient by ClinGen,[35] or LoF-intolerant genes as measured by a high probability of LoF intolerance (pLI) score (>0.9).[20] Conservation of the variant site is reported with the genomic evolutionary-rate profiling (GERP) score.[36] This variant was submitted under accession number ClinVar: SCV000746597.1.

Generation of Fly Stocks

All fly strains used in this study were generated in house or obtained from the Bloomington *Drosophila* Stock Center (BDSC) and cultured at room temperature unless otherwise noted. The $pits^{MI02926\text{-}TG4.1}$ allele was generated by genetic conversion of the MiMIC[37,38] (Minos mediated integration cassette) insertion line, y^1 *w* Mi{MIC}CG11138*^{MI02926} (BDSC_36165) via recombination-mediated cassette exchange (RMCE) as described.[39–41] The recessive lethality associated with the $pits^{MI02926\text{-}TG4.1}$ allele was rescued with an 80 kb P[acman] duplication (*w[1118]; Dp(1;3)DC256, PBac{y[+mDint2] w[+mC] = DC256}VK33*) (BDSC_30373)[42] as well as by a 20 kb genomic rescue construct (see below). We determined the cell-type pattern of *pits* by crossing $pits^{MI02926\text{-}TG4.1}$ to *UAS-mCD8-eGFP* (BDSC_32184). In addition, the y^1 *w* Mi{MIC}CG11138*^{MI02926} line was converted to a protein trap line (Pits::GFP) by injection of a construct that could either produce a splice acceptor (SA)-T2A-GAL4-polyA mutant allele or a SA-eGFP-splice donor (SD) protein trap allele depending on the inserted direction. The

successful generation of the Pits::GFP allele was confirmed by both PCR of genomic DNA and anti-GFP immunohistochemistry and immunoblotting of fly tissue.

All transgenic constructs were generated by Gateway (Thermo Fisher Scientific) cloning into the pUASg-HA.attB plasmid.[43] The human *IRF2BPL* cDNA clone[30] was made to match the GenBank: NM_024496.3 transcript. Flanking Gateway *attB* sites were added by PCR of the template cDNA clone and then shuttled to the pDONR223 by BP clonase II (Thermo Fisher Scientific). Variants were generated by Q5 site-directed mutagenesis (NEB), fully sequenced (Sanger), and finally cloned into pUASg-HA.attB via LR clonase II (Thermo Fisher Scientific). All expression constructs were inserted into the VK37 (*PBac{y[+]-attP}VK00037*) docking site by ϕC31 mediated transgenesis.[44] We generated the 20 kb genomic rescue (GR) line by inserting the P[acman] clone CH322-141N09 (BACPAC Resources)[45] into the VK37 docking site. We generated the *UAS-pits-RC* flies by obtaining the *pits* cDNA (RE41430, RC isoform) clone from the *Drosophila* Genomics Resource Center (DGRC) and performing Gateway (Thermo Fisher Scientific) cloning into pUASg-HA.attB. The *pits* RNAi (RNA interference) line (*P{KK108903}VIE-260B*) was obtained from Vienna *Drosophila* Resource Center (VDRC). The GAL4 lines used in this study from BDSC are *nSyb-GAL4* (y^1 *w*; P{w*$^{+mW.hs}$ = *nSyb-GAL4.S}3*) BDSC_51635, *Rh1-GAL4* (*P{ry*$^{+t7.2}$ = *rh1-GAL4}3, ry*^{506}) BDSC_8691 and *Act-GAL4/CyO* (y^1 *w*; P{w*$^{+mC}$ = *Act5C-GAL4}25FO1/CyO, y*$^+$) BDSC_ 4414.

Drosophila *Behavioral Assays*

For the bang sensitivity assay,[46] flies were anesthetized no sooner than 24 hours prior to being tested with CO_2 and were housed individually. At the time of testing, flies were transferred to a clean vial without food and vortexed at maximum speed for 15 s. The time required for flies to recover to an upright position was measured. Typically, 25 flies were tested per data point. The climbing assay[47] was performed in a similar manner, but at the time of testing flies were transferred to a fresh vial and given 1 minute to habituate before being tapped to the bottom of the vial three times and examined for a negative geotaxis (climbing) response to reach the 7 cm mark on the vial. Flies were given a maximum of 30 s to reach the top.

Histological and ultrastructural analysis of the fly retina: 45-day-old flies were dissected in ice-cold fixative (2% PFA, 2.5% glutaraldehyde, and 0.1 M sodium cacodylate). Heads were fixed, dehydrated, and embedded in Embed-812 resin (Electron Microscopy Sciences) as described previously.[48] Histological sections (200 nm thick) were stained with toluidine blue and imaged with a Zeiss microscope (Axio Imager-Z2) equipped with an AxioCam MRm digital camera. For transmission electron microscopy (TEM), sections (50 nm thick) were stained with 1% uranyl acetate and 2.5% lead citrate. TEM images were obtained with a transmission electron microscope (model 1010, JEOL). Images were processed with Photoshop (Adobe), and 45-day-old toluidine blue images were color matched to the 5-day-old images for clarity.

Overexpression of Human IRF2BPL *in* Drosophila

We overexpressed reference and variant *IRF2BPL* cDNA molecules in flies by crossing the *UAS-IRF2BPL* males to virgin female flies from a ubiquitous (*Act-GAL4*) driver stock. The progeny of these crosses were cultured at various temperatures (18°C, 22°C, 25°C, and 29°C) so that the human proteins were expressed at different levels (lowest expression at 18°C and highest expression at 29°C).[38,49] Flies were assessed for the expected Mendelian ratios. For temperatures ≥22°C, more than 100 flies were assessed for each cross. For 18°C crosses, more than 50 flies were assessed from each group.

For additional methods, please see the Supplemental Data.

Results

Summary of Clinical Findings

The subjects described in this series are between 2.5 and 43 years of age and include one subject who died at 15 years of age. Comprehensive clinical information is included in the Supplemental Note, Table S1, and Table S2.

All seven individuals have heterozygous variants in *IRF2BPL* (Table 1 and Table S1). All variants have been confirmed by Sanger sequencing. The variants were *de novo* in all for whom parental testing was available (five out of seven subjects) (Table1). The nonsense variants identified in *IRF2BPL* (GenBank: NM_024496.3) are c.376C>T (p.Gln126*), c.379C>T (p.Gln127*), c.514G>T (p.Glu172*), and c.562C>T (p.Arg188*) (the latter was identified in two individuals). There was remarkable similarity in the clinical course of the five individuals that had nonsense variants. These include an unremarkable course of initial development, followed by loss of developmental milestones and development of a pediatric-onset seizure disorder at a variable age, with 2 years being the earliest age of onset. Additional findings included a movement disorder with dystonia and choreoathetosis, as well as cerebellar signs such as ataxia, dysarthria, dysmetria, and dysdiadochokinesia. Three of the probands had anomalies of eye movements but had normal retinae and optic nerves. Head circumference appeared to remain appropriate for age in those with available measurements. Brain MRI was normal early in life, but cerebral and cerebellar atrophy was noted in the two oldest subjects (Figure 2). Cognitive status was difficult to assess, particularly because verbal skills were lost. However, cognitive abilities appeared to remain intact over a short follow-up period in one subject and to deteriorate in an older individual. One individual passed away at 15 years of age when the family elected to limit care after continued decline.

Missense variants c.1115C>G (p.Pro372Arg) and c.1254G>C (p.Lys418Asn) were also reported in *IRF2BPL* in two individuals who had a variable phenotype of global developmental delay and seizures. The older individual (subject 6) had a diagnosis of ASD. Despite intractable epilepsy, subject 7 was eventually weaned off antiepileptic drugs, and seizures did not recur over a short follow-up period. In both individuals, *IRF2BPL* variants were *de novo*. Neither individual has developed a progressive loss of milestones, abnormal eye movements, or a movement disorder at 2 and 10 years of age.

IRF2BPL De Novo Variants Are Deleterious according to Bioinformatics Data

IRF2BPL is a gene that is highly intolerant to variation; it has a residual variation intolerance score (RVIS)[50] of 9.3%

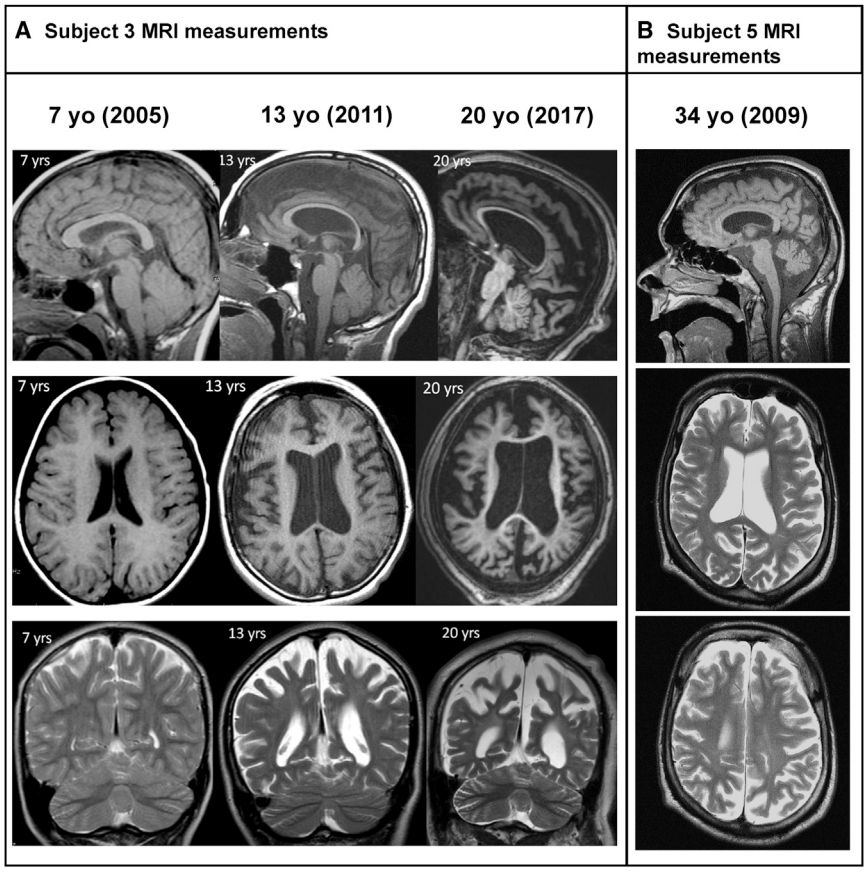

Figure 2. Progressive Cerebral Atrophy in Individuals with *IRF2BPL* Nonsense Truncations

(A) Brain MRI for subject 3 at 7, 13, and 20 years (top row, axial FLAIR; bottom row, sagittal T1). Brain MRI was normal at 7 years. However, at age 13, there was severe diffuse cerebral atrophy with *ex vacuo* dilatation of the lateral ventricles. There might be a slightly increased white matter signal in the peritrigonal region, but otherwise the white matter appears intact and does not suggest a leukodystrophy. The cerebellum has only minimal atrophy. There is mild atrophy of the basal ganglia and brainstem (not shown). At age 20 years, there is further atrophy, including severe volume loss in the bilateral cerebral hemispheres, further thinning of the corpus callosum, mild worsening of the increased white matter signal in the peritrigonal region, and further atrophy of the cerebellum and brainstem.

(B) MRI of subject 5 at 34 years depicts global cerebral and cerebellar atrophy, thinning of the corpus callosum and brainstem, and no focal brain lesions (axial T2-weighted and sagittal T1-weighted). Images were taken on a 1.5T Siemens magnetic resonance system.

and a pLI score of 0.97, with no observed LoF variants included in the calculation.[20] The only LoF variants present in ExAC and gnomAD are frameshifts, which either do not pass quality filtering or appear to be artifactual calls in repetitive regions when the browser visualization tool is used.[20] *IRF2BPL* is also constrained to missense variants ($z = 4.73$).[20] All variants found in the subjects were absent from the gnomAD and ExAC databases. The combined annotation-dependent depletion (CADD)[51] score for all of the variants was >34, which places them among the variants predicted to be most deleterious. To determine the relative representation of *IRF2BPL de novo* variants in our collective baseline patient population of sequenced individuals with neurodevelopmental phenotypes, we used fitDNM to calculate a p value for the confirmed *de novo* variants (three nonsense and two missense in a total of 8,961 exomes performed for neurodevelopmental phenotypes). fitDNM[52] simultaneously considers whether there is enrichment for *de novo* LoF and missense variants within in a gene in an affected population (beyond what is expected) and also weights these variants by the predicted damaging properties. We found there was a significant enrichment for *de novo* damaging variants in *IRF2BPL* within the neurodevelopmental phenotype cohort ($p = 4.36 \times 10^{-7}$), and when corrected for the 18,892 genes in the Consensus Coding Sequence Project (CCDS release 20), the results maintain significance ($p = 0.008$).[52] The four nonsense variants introduce a premature termination codon either downstream (Glu172 and Arg188) or at the end (Gln126 and Gln127) of the poly-glutamine tract and upstream of the first PEST sequence (Figure 1A), whereas the missense variants are within the variable region of the protein. We used the DOMINO tool to assess the likelihood of monoallelic variants in *IRF2BPL* to cause a Mendelian disease. *IRF2BPL* had a DOMINO score of 0.962 out of 1, predicting that monoallelic variants would most likely cause disease (Figure 1B).[53]

Functional Assays in Flies Indicate that *IRF2BPL* Variants Are Severe Loss-of-Function Mutations

To validate the functional consequences of these variants, we utilized *Drosophila melanogaster* as a model organism. Experiments in fruit flies have previously provided experimental support in identifying causal variants for human disease,[19,54–56] and these approaches have been an integral part of the UDN.[13,14,16,21,57] The fly ortholog of *IRF2BPL* is a poorly characterized gene, *CG11138*. This gene was studied in the context of epigenetic regulation through biochemical methodologies during embryogenesis and was named *pits* (*protein interacting with Ttk69 and Sin3A*).[58] Although the overall identity (30%) and similarity (36%) between IRF2BPL and Pits may not seem high, the architecture of the protein is very similar, and the

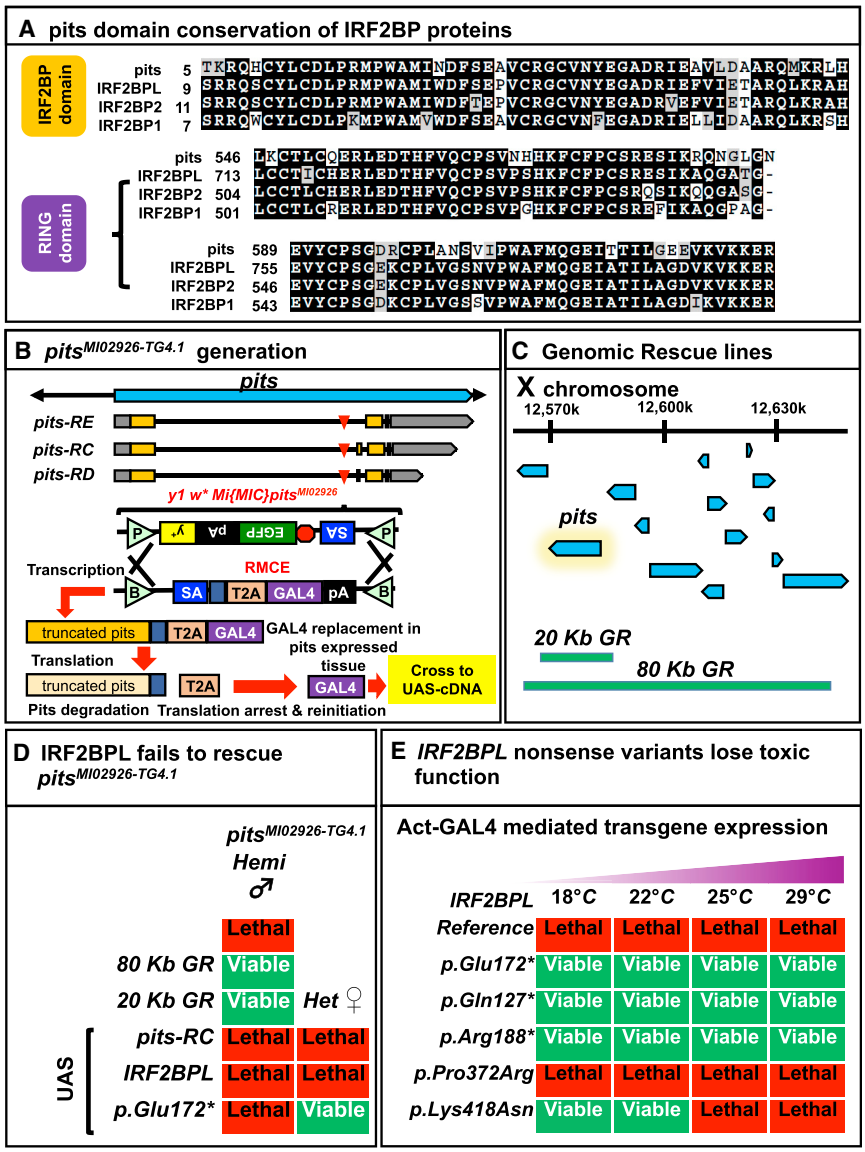

Figure 3. The IRF2BPL Ortholog, Pits, Is Highly Conserved, and Human Disease Variants Display a Dramatic Loss of Function

(A) The two annotated domains (IRF2BP zinc finger and C3HC4 RING finger) for IRF2BPL (as well as IRF2BP1 and IRF2BP2) display very high conservation with the fly ortholog Pits.

(B). The *pits*$^{MI02926\text{-}TG4.1}$ allele was generated by genetic conversion of y^1 *w* Mi{MIC}CG11138*^{MI02926} by recombination-mediated cassette exchange (RMCE) *in vivo*. The resulting mutant incorporates a SA-T2A-GAL4, which acts as an artificial exon and results in early truncation of the *pits* transcript and cellular replacement with GAL4 expression under the endogenous pits regulatory elements.

(C) Genomic location of genomic rescue (GR) constructs inserted on chromosome 2 (VK37) of the fly. Note that the 20 kb rescue line is only specific for *pits*.

(D) Reintroduction of either GR construct (Figure 3C) rescues lethality for *pits*$^{MI02926\text{-}TG4.1}$ flies, but rescue is not observed with overexpression of the fly or human cDNA. Female *pits*$^{MI02926\text{-}TG4.1}$ */FM7* virgins were crossed to males of either GR or UAS lines, and progeny were examined for males containing *pits*$^{MI02926\text{-}TG4.1}$ and the rescue construct (minimum progeny examined n = 91). Examination of female flies heterozygous for the presence of *pits*$^{MI02926\text{-}TG4.1}$ and the rescue construct revealed a lack of toxicity in female *pits*$^{MI02926\text{-}TG4.1}$ */+; UAS-IRF2BPL-Glu172*/+* flies, indicating a loss of function.

(E) The ubiquitous expression of *UAS-IRF2BPL* or variants with *Act-GAL4* reveals that all nonsense variants are strong loss-of-function mutations and that the p.Lys418Asn causes partial loss of function.

sequences of the annotated domains show high conservation (79% identity for the zinc-finger domain, 76% identity for the C3HC4 RING domain) (Figure 3A). Pits also has a DIOPT[59] score of 12/15, suggesting that *pits* is likely to be a true ortholog of *IRF2BPL*. Two other human paralogs of *IRF2BPL* share a similar high DIOPT score (12/15 for *IRF2BP1*; 11/15 for *IRF2BP2*). These data indicate that *pits* is the sole fly gene that is orthologous to the three *IRF2BP* family genes in humans.

To generate a *pits* mutant fly, we used a MiMIC insertion in a *pits* intron, named *Mi{MIC}CG11138*^{MI02926} (Figure 3B).[37,38] MiMICs are engineered transposable elements that contain inverted *attP* sites derived from phage ΦC31 flanking a swappable cassette. This allows replacement of the content of the *MiMIC* insertion via recombination-mediated cassette exchange (RMCE) by expression of the ΦC31 integrase so that the *MiMIC* cassette is swapped with a *SA-T2A-GAL4-polyA* (T2A-GAL4) cassette.[39–41] This insertion results in a truncated *pits* transcript because of the polyA signal. During translation, this short transcript produces a short protein that is truncated at the T2A site yet allows re-initiation of translation to produce the GAL4 protein. The GAL4 protein is detected in a proper spatial and temporal fashion, i.e., those of the endogenous gene[38] (Figure 3B). This allows rescue of the *T2A-GAL4* induced allele, typically a null allele, with a UAS-(fly) cDNA for about 70% of the genes tested.[40]

The *pits* gene is on the X chromosome, and *pits*$^{MI02926\text{-}TG4.1}$ males are hemizygous lethal; they fail to survive past the first instar larval stage, and most die as embryos. Lethality can be rescued so that males survive to viable adults by introduction of an 80 kb or a 20 kb P[acman] genomic BAC rescue (GR) construct, the latter only carrying the *pits* gene[42,44] (Figures 3C and 3D). Hence, *pits* is an essential gene, and expression of the gene in the proper genomic context fully rescues the LoF of *pits*.

We attempted to rescue lethality observed in *pits*$^{MI02926\text{-}TG4.1}$ flies by overexpression of *UAS-pits* or *UAS-IRF2BPL* and failed to obtain viable flies. Intriguingly, we were also unable to obtain viable heterozygous female flies that contain both the *pits*$^{MI02926\text{-}TG4.1}$ allele and *UAS-pits* or *UAS-IRF2BPL* (Figure 3D). These data show that overexpression of the fly or human IRF2BPL in the cells that endogenously express Pits is toxic to the fly. Indeed, expression of *UAS-IRF2BPL* under the control of a ubiquitous driver (*Act-GAL4*) also causes lethality (Figure 3E).

The above data show that the lethality caused by overexpression of the reference *IRF2BPL* gene can be used as a functional assay to test whether the variants are functional (toxic) as well. To modulate the levels of expression, we ubiquitously expressed the variants with *Act-GAL4* because the *UAS-cDNA* expressed with this driver exhibits temperature dependence, whereby there is significantly greater expression at higher temperatures.[38,49] We conducted these experiments at 18°C, 22°C, 25°C, and 29°C. Expression of the reference *IRF2BPL* cDNA consistently causes lethality at all temperatures tested, whereas the three nonsense variants (p.Glu172*, p.Gln127*, and p.Arg188*) consistently produced viable animals at all temperatures tested (Figure 3E). This provides evidence that the truncated proteins are not toxic and are most likely LoF alleles. Interestingly, the missense variant p.Lys418Asn is lethal when expressed at higher temperatures, whereas the flies are viable at lower temperatures, indicating that this variant retains some toxic function and hence behaves as a partial LoF allele. The p.Pro372Arg variant remained lethal upon ubiquitous expression, even at lower temperatures, indicating that its toxic function is similar to that of the reference protein, at least in this assay. We confirmed that the UAS-driven human cDNA in flies expresses IRF2BPL at relatively similar levels by making HA-tagged constructs for the reference and p.Glu172* truncation variants and performing immunoblot analysis, for which we used an anti-HA antibody because commercially available antibodies for IRF2BPL recognize epitopes downstream of the premature termination codon, in the C terminus of IRF2BPL. UAS expression of these constructs in neurons by *nSyb* (neuronal Synaptobrevin)-*GAL4* was relatively similar (Figure S2A). Additionally, we confirmed that the untagged reference and two missense variants had similar amounts of protein by using a commercial antibody against IRF2BPL and performing immunoblot analysis, which suggested that the reduced toxicity of p.Lys418Asn is not due to destabilization of the protein (Figure S2B).

Pits Is Localized and Required in the CNS

To examine the endogenous amounts of Pits as well as its subcellular localization, we generated a GFP protein trap line of *pits*. We integrated a protein trap (splice acceptor [SA]-linker-eGFP-linker-splice donor [SD]) cassette into *pits*^{MI02926} via RMCE. Although SA-eGFP-SD functions as an artificial exon in the middle of *pits* (Figure S3A) and could lead to a non-functional protein, Pits::GFP flies are viable in the homozygous state and do not display any obvious phenotype. This is in concert with our previous findings that most (75%) proteins tolerate the presence of an internal GFP incorporated by SA-eGFP-SD MiMIC insertions.[38] The GFP fusion proteins also reflect the localization of the endogenous proteins.[37,38] We first confirmed the presence of a single protein of the appropriate size via SDS-PAGE in males (Figure 4A). As shown in Figures 4B and 4C, the tagged protein is widely detected in the brain. In the third-instar larval brain, the protein is widely detected and is enriched in the mushroom body (MB, Figure 4B, yellow arrow). In the adult brain, Pits::GFP is localized in most neurons, including the cell bodies and nuclei (co-staining with a pan-neuronal nuclear marker, Elav) of many neurons as well as their axons (Figure 4C). This is in agreement with a previous study showing that *pits* is localized to the nucleus.[60] Pits::GFP is not detected in the glia of the adult CNS upon pan-glial staining with Repo (Figure S3B). Additionally, we also determined the cell-type pattern of Pits by using the GAL4 reporter from *pits*$^{MI02926\text{-}TG4.1}$ allele crossed to a UAS-membrane-bound GFP (Figure S3C), which allows detection of cells that express the gene of interest at low levels.[40] We also generated confocal images (z stacks) of Pits::GFP brains co-stained with Elav (Video S3) and Repo (Video S4). These data reveal that Pits is enriched in the MB, the learning and memory center of the flies,[61] as well as in the antennal mechanosensory and motor center, which are required for balance and hearing and motor coordination, a cerebellar insect equivalent.[62] Again, no Pits was detected in glia from these analyses.

Because of the lethality observed in *pits*$^{MI02926\text{-}TG4.1}$ flies, we determined the function of Pits in the brain through gene-knockdown studies using RNAi.[63] Ubiquitous knockdown of *pits* with *Act-GAL4* resulted in semi-lethality (Figure 5A). *UAS-pits-RNAi* has specificity to *pits* in that it consistently reduces the endogenous amount of Pits to ~50% of *UAS-luciferase-RNAi* when assessed via immunoblot (Figure 5B). To determine whether partial knockdown of *pits* results in neurological defects, we expressed *UAS-pits-RNAi* with the *nSyb-GAL4* driver. Young flies (~5 days after eclosion) displayed normal climbing (Figure 5C) and mechanical stress tolerance (bang sensitivity) (Figure 5D). However, aged flies that were 30 and 45 days past eclosion displayed progressive abnormalities in climbing and became bang sensitive at 30 days after eclosion in comparison to controls (Figures 5C and 5D).

To determine whether an age-dependent deterioration in neural morphology could be observed, we reduced *pits* expression in photoreceptors of the fly eye by using rhodopsin (*Rh1*)-*GAL4*. The fly retina is a well-characterized system useful for exploring neurodegeneration in *Drosophila* as a result of the highly stereotypical organization of neurons (photoreceptors) and glia cells (pigment cells, cone cells) in this tissue.[19,55] Indeed, Pits::GFP shows a robust nuclear signal in the photoreceptors of the fly retina when the retina is co-stained with Elav (Figure S4).

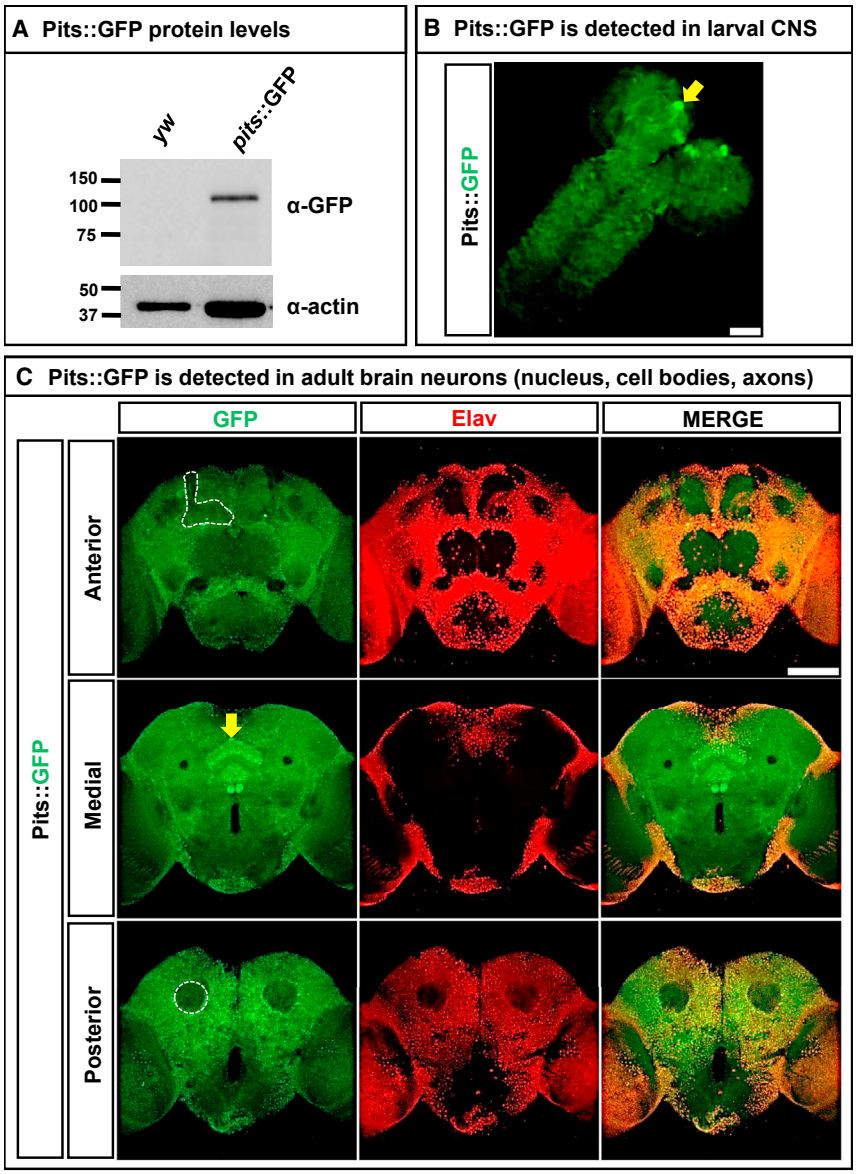

Figure 4. The *IRF2BPL* Ortholog, *pits*, Is Localized to Both the Developing and Adult CNS and Is Present in the Nucleus of a Wide Subset of Neurons

(A) Male fly heads were lysed and run on SDS-PAGE to determine the presence of Pits::GFP.

(B) Pits was widely detected in third-instar larvae, assessed by immunostaining of homozygous Pits::GFP animals, and viewed by confocal microscopy (z stack—max projection). Note the enrichment in the mushroom body (yellow arrow).

(C) Single-slice confocal images of the adult CNS show that *pits* is localized to neurons (co-localized with Elav). Notably, *pits* is detected in the cell bodies of the adult mushroom body (top left panel), is enriched in the central complex (yellow arrow), and is not present in the dendrites of the mushroom body (bottom left panel). The scale bar represents 50 μm.

Flies were raised in a 12 hr light/dark cycle for 45 days, and histological examination of retina sections stained with toluidine blue was performed. We observed a severe disorganization of the ommatidia (units of photoreceptors) and notable rhabdomere (light-sensing organelle) loss (Figure 6A). This loss was not observed in young flies (5 days after eclosion), nor in aged control RNAi flies. To examine ultrastructure, we performed transmission electron microscopy (TEM) of the same tissue and observed numerous abnormalities in the ultrastructure of the *Rh1-GAL4 > pits-RNAi* retina compared to age-matched *Rh1-GAL4 > control-RNAi* eyes (Figures 6B and 6C and Figures S5 and S6): (1) a significant decrease in intact rhabdomeres (Figure 6D); (2) a significant increase in the presence of tubulovesicular-like structures (TVSs), associated with some neurodegenerative models[64,65] (Figure 6C, red arrow); and (3) the abnormal presence of neuronal lipid droplets in photoreceptors (Figure 6C, yellow arrow; Figure S7A), often associated with mutants that cause high accumulation of reactive oxygen species (ROS).[66] However, we did not detect obvious changes in mitochondrial morphology or the number of mitochondria per photoreceptor (Figure S7B). In summary, *pits* is required for proper maintenance of neuronal function and structure in flies.

Discussion

We present seven subjects with rare heterozygous variants in *IRF2BPL*, a gene that has not previously been associated with disease in humans. The subjects with nonsense variants exhibited a remarkably similar, progressive course of neurological regression that eventually led to severe developmental disability. In contrast, the missense variants observed in two subjects are associated with milder neurological symptoms such as seizures, developmental delay, and ASD. Interestingly, the nonsense variants in this cohort cluster in or just downstream of the polyglutamine tract within the variable region, whereas the missense variants map farther downstream (Figure 1A). The bioinformatics signature of the gene suggests that *IRF2BPL* is highly intolerant to variation and that the variants reported in the cohort are among the most deleterious. We demonstrated that *IRF2BPL de novo* predicted damaging variants are overrepresented in individuals with neurodevelopmental phenotypes. The DOMINO score was suggestive of dominant inheritance. RNA sequencing from a blood sample for subject 1 (c.514G>T [p.Glu172*]) revealed expression of the

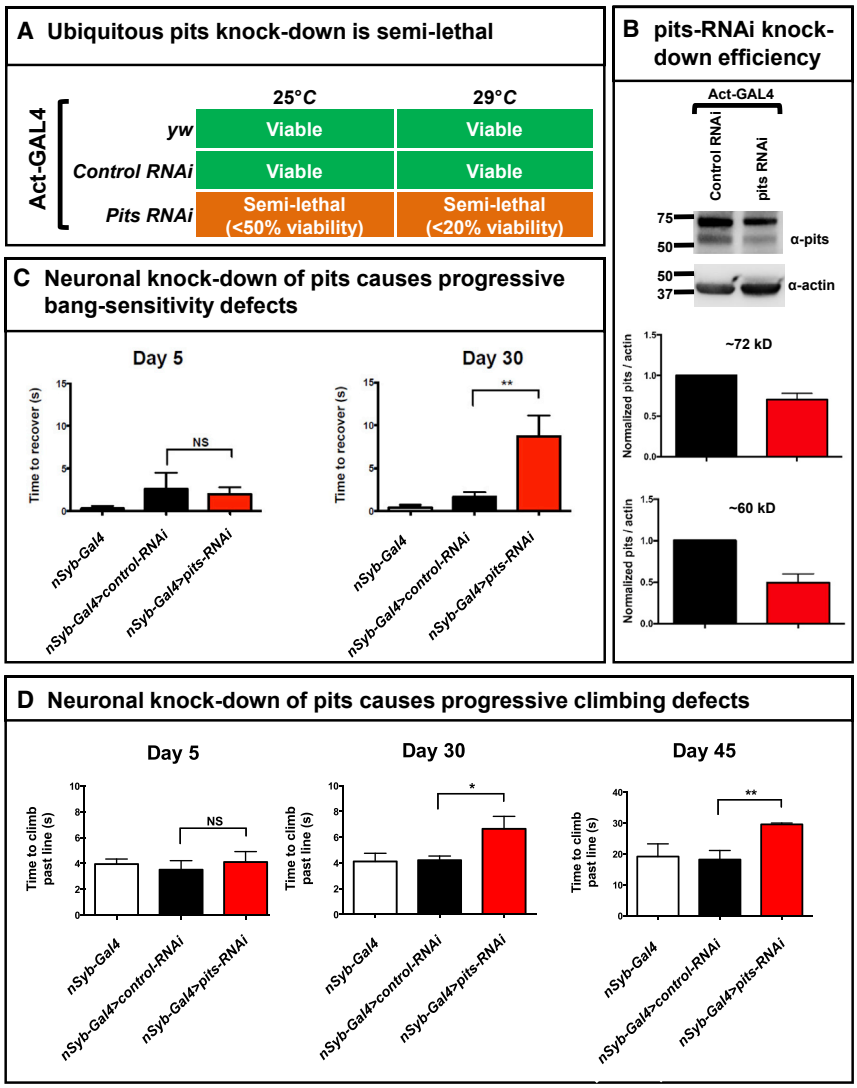

Figure 5. Neuronal Knockdown of *pits* Leads to Progressive Behavioral Deficits

(A) Ubiquitous knockdown of *pits* results in semi-lethality, as shown by lower-than-expected genotypic ratios of survival into adulthood. *Act-GAL4 > UAS-pits-RNAi* flies were compared to *Act-GAL4 > control-RNAi* (*control-RNAi = UAS-luciferase-RNAi*) and the *Act-GAL4* driver alone (with no *UAS*).

(B) *Act-GAL4 > UAS-pits-RNAi* can partially knock down ~50%–60% of the *pits* isoforms consistently observed in female flies. The two isoforms observed have been previously documented.[59]

(C) Pan-neuronal knockdown of *pits* (*nSyb-GAL4 > UAS-pits-RNAi*) leads to a bang-sensitive paralytic phenotype in aged animals. This phenotype is not observed in control flies (*nSyb-GAL4* alone or *nSyb-GAL4 > UAS-luciferase-RNAi*) or young animals. Multiple cohorts of flies were anesthetized and singly housed 24 hours prior to testing with 15 s of vortexing in an empty vial. Statistical analyses were with one-way ANOVA followed by a Tukey post-hoc test. Results are means + SEM (*$p < 0.05$; NS, not significant)

(D) Pan-neuronal knockdown of *pits* (*nSyb-GAL4 > UAS-pits-RNAi*) leads to progressive climbing deficits that are only observed in aged flies. Singly housed flies (similar to above) were given 1 minute to habituate to an empty vial before being tapped three times. Flies were given 30 s to cross the 7 cm mark on the vial. Flies that failed to cross the line were given a score of 30 (only seen at day 45). One-way ANOVA was followed by a Tukey post-hoc test. Data are means + SEM (*$p < 0.05$, **$p < 0.01$; NS, not significant).

transcript (data not shown). The lack of nonsense-mediated decay of *IRF2BPL* transcript with a nonsense mutation is consistent with the fact that this is a single-exon gene.[67] Immunoblotting on subject samples with nonsense variants could not be pursued because a commercially available antibody that recognizes an epitope upstream of the premature truncations was not available.

To date, understanding of a role for *IRF2BPL* in humans has been limited to an association with developmental phenotypes. For example, *IRF2BPL* has been identified in the top 1,000 genes that are significantly lacking in functional coding variation in non-ASD samples and are enriched with *de novo* LoF mutations identified in cases of ASD.[68] Other large-scale sequencing studies have identified *de novo* variants in *IRF2BPL* in ASD (two individuals) and major developmental disorders (two individuals) (Figure 1A).[1,3] Intriguingly, the ASD variants include a missense variant in the conserved DNA-binding domain (c.90C>G [p.Phe30Leu]) and a frameshift variant near the end of the protein (c.2102del1 [p.Asn701Thrfs*66]). The respective verbal and non-verbal IQs of the individuals with the ASD-implicated missense (24, 41) and frameshift (83, 74) variants are below average. The developmental-disorder cohort also has a missense variant (c.1171C>T [p.Arg391Cys]) and a frameshift that similarly occurs near the end of the protein (c.2138del1 [p.Leu713Profs*54]).[1,3] The missense variants in these individuals compared to our two subjects indicate that an understanding of the full spectrum of IRF2BPL-related phenotypes is still developing. The p.Asn701Thrfs*66 frameshift, in particular, suggests that truncations near the end of the protein might cause variable phenotypes. Another possibility is the presence of mosaicism in these large cohort studies. Several copy-number variants, including three deletions, have been identified in the DECIPHER database.[69] Phenotypic information is available for only one subject that had a paternally inherited deletion of 1.39 Mb along with autistic behavior, cognitive impairment, and seizures. The size of the copy-number variants varies from 185 kb to 19.7 Mb, and all are described as

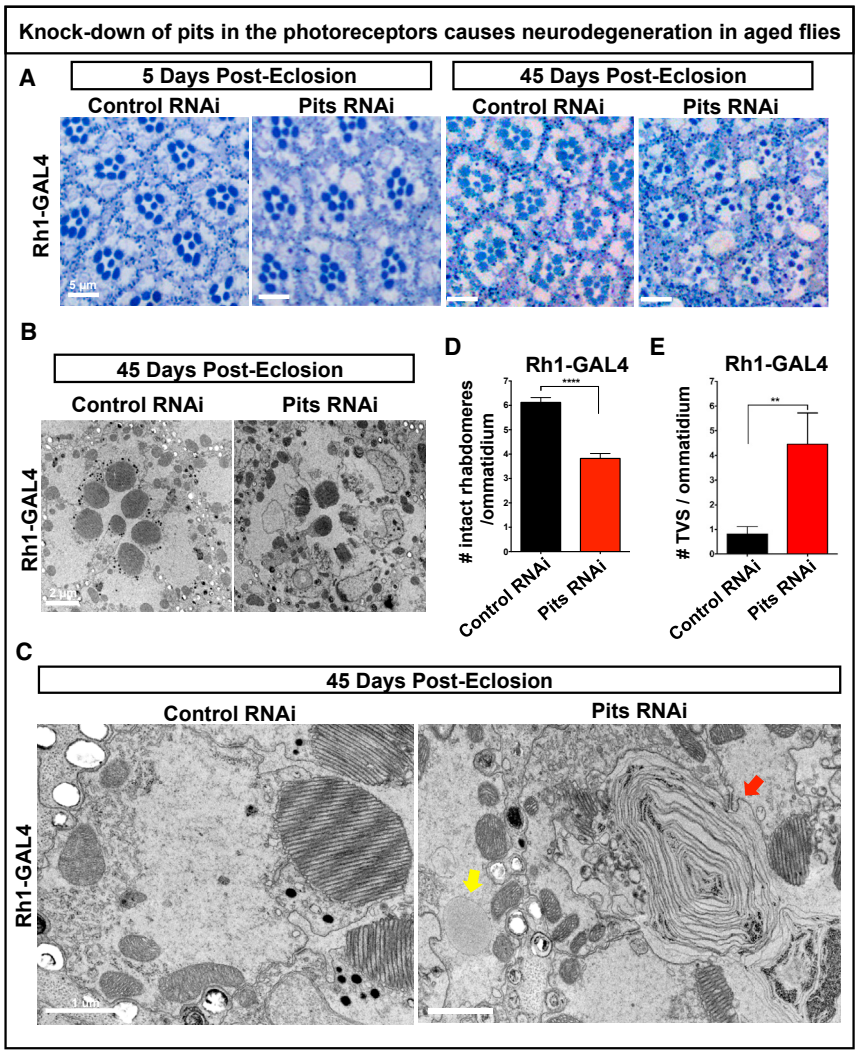

Figure 6. Knockdown of *pits* in the Photoreceptor Leads to Degenerative Phenotypes in Aged Animals

(A) Toluidine blue staining of 5- and 45-day-old retina from control (*Rh1-GAL4 > UAS-luciferase-RNAi*) and *Rh1-GAL4 > Pits-RNAi* (*Rh1-GAL4 > UAS-pits-RNAi*) flies reveals disorganization of the ommatidtia and photoreceptor loss. The scale bar represents 5 μm.

(B and C) TEM images showing the photoreceptors and the ommatidia (scale bar in B represents 2 μm) and photoreceptor (scale bar represents 1 μm in C) section. The red arrow indicates the presence of tubulovesicular-like structures (TVSs), and the yellow arrow indicates neuronal lipid droplets (C). Further TEM images are available in Figures S5 and S6.

(D and E) Quantification of rhabdomere loss (D) and TVSs (E) on a minimum of n = 27 randomized sections from the retina from three animals per genotype. Statistical analyses were with unpaired two-tailed t tests. Results are means + SEM (**$p < 0.01$, ****$p < 0.0001$).

having uncertain significance to the phenotype. Given the size and inclusion of multiple genes, it would be difficult to speculate on a discrete role for *IRF2BPL* in the phenotypes.

Our findings offer additional evidence that variants in *IRF2BPL* are implicated in neurological symptoms, and they additionally extend the phenotype into neurodevelopmental regression. Furthermore, our model-organism experiments with fruit flies support an important role for *IRF2BPL* in embryologic development as well as neuronal maintenance. *IRF2BPL* is well conserved, and the fly gene, *pits*, is abundant in the nervous system during development and in adulthood. The $pits^{MI02926\text{-}TG4.1}$ LoF mutants fail to survive past early larval stages and mostly die as embryos. Although we were not able to rescue the $pits^{MI02926\text{-}TG4.1}$ allele with either the human or fly cDNA, $pits^{MI02926\text{-}TG4}$ is rescued with a genomic rescue construct specific to *pits*, showing that this chromosome does not carry other lethal or second-site mutations. Interestingly, ubiquitous overexpression of *IRF2BPL* or *pits* in flies is toxic, suggesting that the gene is highly dosage sensitive. Many genes implicated in neurodegenerative disorders cause overexpression phenotypes in *Drosophila*.[70,71] In our experiments, however, overexpression of the nonsense variants was not toxic. These results suggest that the mechanism of disease might be through a loss of protein function of *IRF2BPL*. Overexpression of the missense variants showed a range of effects. Although overexpression of p.Lys418Asn was only lethal at higher temperatures (i.e., higher levels of expression), p.Pro372Arg was lethal at any temperature. These results suggest that some of the proteins with the missense variants retained a toxic function when overexpressed. Understanding the precise molecular function of Pits and IRF2BPL will allow researchers to design experiments to test this possibility. In summary, either excess or loss of *pits* or *IRF2BPL* is highly detrimental to survival. The fact that expression at low levels (*Act-GAL4* at 18°C) is still toxic suggests that expression of the gene product is highly regulated *in vivo* through mechanisms such as ubiquitination through the PEST domain. Note that the truncating variants in *IRF2BPL* might produce a peptide that could aggregate and mislocalize. The nonsense variants cluster around the polyQ stretch and might produce a toxic protein. However, neuronal overexpression of these truncated variants in aged flies causes no obvious phenotypes, suggesting that they are not highly toxic.

Although RNAi knockdown of *pits* might not be an ideal model for truncating variants in *IRF2BPL*, phenotypic similarities between a partial Pits reduction in flies and symptoms observed in humans suggest evolutionary conservation in neuronal mechanisms. For example, (1) all

individuals had seizures or EEG abnormalities, and a reduction of Pits in neurons led to a bang-sensitive phenotype in flies. Bang-sensitivity is associated with seizure-like paralysis that has phenotypic as well as genetic parallels with human epilepsy.[72,73] (2) The five individuals carrying nonsense variants in *IRF2BPL* displayed progressive motor dysfunction that manifested after early childhood. Similarly, neuronal reduction of Pits in flies caused a progressive decline in climbing ability that was not observed in young flies. (3) The two oldest individuals, who have nonsense variants, display cerebral atrophy in adulthood. Correspondingly, we found that a reduction in *pits* expression in photoreceptors led to a slow and age-dependent loss of neuronal integrity. (4) The cerebellar symptoms and cerebellar atrophy might correspond to a requirement for *pits* expression in the antennal mechanosensory and motor center. These neurons are required for balance and auditory and motor coordination, the insect equivalent of the cerebellum,[62] and Pits is abundant in these cells. These results support the notion that IRF2BPL and Pits have fundamental roles in the development and maintenance of the CNS.

IRF2BPL has similarity to its mammalian paralogs IRF2BP1 and IRF2BP2 and has been shown to interact with IRF2 (interferon regulatory factor 2).[74,75] However, flies lack an obvious homolog to IRF2, indicating that *pits* and *IRF2BPL* might have additional conserved functions that are currently unknown. Recently, a study in *Drosophila* indicated that the fly ortholog, Pits, regulates transcription during early embryogenesis by interacting with a histone deacetylase, Sin3A (SIN3A and SIN3B in humans) and a co-repressor, Tramtrack 69 (no identified human ortholog).[58] Consistent with previous studies in flies and rats, our data suggest that both Pits and IRF2BPL are found predominantly in the nucleus.[60,76] We showed enrichment in the nucleus of photoreceptors and numerous neurons, but we also observed Pits::GFP in axons and cell bodies and little to no staining in the dendrites of the mushroom body. This could indicate that Pits might have a non-nuclear role in specific subcellular compartments in neurons. Finally, through neuron-specific knockdown experiments in flies, we demonstrate that *pits* is important for function and/or neuronal maintenance over time.

Within the cohort, we observed different phenotypes according to the type of variant. All four nonsense variants truncate IRF2BPL upstream of the putative nuclear localization signal, the conserved C-terminal RING domain, and multiple putative PEST sequences. Although little is known about IRF2BPL and Pits, most studies implicate their localization and function in the nucleus.[30,58,60,76,77] However, the RING domain of IRF2BPL has recently been shown to act as an E3-ligase that ubiquitinates β-catenin and suppresses Wnt signaling in gastric cancer.[32] It is currently unclear whether this pathway might be altered in IRF2BPL-associated disease. Finally, the predicted PEST sequences suggest that IRF2BPL is highly regulated and support our data indicating that overexpression of the protein can be detrimental. Toxicity was observed by overexpression of fly or human cDNA constructs in all cells (*Act-GAL4*) or within the cell types in which *pits* is endogenously expressed ($pits^{MI02926\text{-}TG4.1}$). Although *IRF2BPL* ubiquitous expression or overexpression within the cell types in which *pits* is endogenously expressed caused lethality, we did not observe lethality or any remarkable phenotypes by overexpression of *IRF2BPL* or the variants when *IRF2BPL* was expressed specifically in neurons (*nSyb-GAL4*) (data not shown). Therefore, increased abundance of Pits and IRF2BPL might be detrimental only to certain cells. Our functional assays of nonsense and missense variants support loss of function and tight control of protein expression and/or turnover. Future studies will aim to determine IRF2BPL targets for ubiquitination and binding partners that mediate neurological phenotypes.

In summary, we have implicated dominant *de novo* variation in *IRF2BPL* to a neurological disorder in humans. We observed that individuals with nonsense variants in this single-exon gene suffer from a progressive and devastating neurological regression, and individuals with rare missense variants also show a spectrum of neurological phenotypes. The bioinformatics signature supports a deleterious effect in IRF2BPL at the gene and variant levels. We provide functional analysis in flies to support a loss-of-function model of *IRF2BPL*-associated disease. Future studies examining the mechanism of early death in *pits*-mutant flies, as well as molecular mechanisms of neurodegeneration in *pits*-knockdown animals, will most likely shed light on conserved pathways essential for neurological development.

Accession Numbers

The accession number for the *IRF2BPL* cDNA sequence reported in this paper is GenBank: NM_024496.3. The accession number for the *pits* cDNA sequence reported in this paper is GenBank: AY119139.1.

Supplemental Data

Supplemental Data include a Supplemental Note, Figures S1–S7, Tables S1–S3, and Videos S1–S4 and can be found with this article online at https://doi.org/10.1016/j.ajhg.2018.07.006.

Consortia

The Program for Undiagnosed Diseases (UD-PrOZA) co-investigators are Steven Callens, Paul Coucke, Bart Dermaut, Dimitri Hemelsoet, Bruce Poppe, Wouter Steyaert, Wim Terryn, and Rudy Van Coster.

The Undiagnosed Diseases Network co-investigators are David R. Adams, Mercedes E. Alejandro, Patrick Allard, Mahshid S. Azamian, Carlos A. Bacino, Ashok Balasubramanyam, Hayk Barseghyan, Gabriel F. Batzli, Alan H. Beggs, Babak Behnam, Anna Bican, David P. Bick, Camille L. Birch, Devon Bonner, Braden E. Boone, Bret L. Bostwick, Lauren C. Briere, Donna M. Brown, Matthew Brush, Elizabeth A. Burke, Lindsay C. Burrage, Shan

Chen, Gary D. Clark, Terra R. Coakley, Joy D. Cogan, Cynthia M. Cooper, Heidi Cope, William J. Craigen, Precilla D'Souza, Mariska Davids, Jyoti G. Dayal, Esteban C. Dell'Angelica, Shweta U. Dhar, Ani Dillon, Katrina M. Dipple, Laurel A. Donnell-Fink, Naghmeh Dorrani, Daniel C. Dorset, Emilie D. Douine, David D. Draper, David J. Eckstein, Lisa T. Emrick, Christine M. Eng, Ascia Eskin, Cecilia Esteves, Tyra Estwick, Carlos Ferreira, Brent L. Fogel, Noah D. Friedman, William A. Gahl, Emily Glanton, Rena A. Godfrey, David B. Goldstein, Sarah E. Gould, Jean-Philippe F. Gourdine, Catherine A. Groden, Andrea L. Gropman, Melissa Haendel, Rizwan Hamid, Neil A. Hanchard, Lori H. Handley, Matthew R. Herzog, Ingrid A. Holm, Jason Hom, Ellen M. Howerton, Yong Huang, Howard J. Jacob, Mahim Jain, Yong-hui Jiang, Jean M. Johnston, Angela L. Jones, Isaac S. Kohane, Donna M. Krasnewich, Elizabeth L. Krieg, Joel B. Krier, Seema R. Lalani, C. Christopher Lau, Jozef Lazar, Brendan H. Lee, Hane Lee, Shawn E. Levy, Richard A. Lewis, Sharyn A. Lincoln, Allen Lipson, Sandra K. Loo, Joseph Loscalzo, Richard L. Maas, Ellen F. Macnamara, Calum A. MacRae, Valerie V. Maduro, Marta M. Majcherska, May Christine V. Malicdan, Laura A. Mamounas, Teri A. Manolio, Thomas C. Markello, Ronit Marom, Julian A. Martínez-Agosto, Shruti Marwaha, Thomas May, Allyn McConkie-Rosell, Colleen E. McCormack, Alexa T. McCray, Matthew Might, Paolo M. Moretti, Marie Morimoto, John J. Mulvihill, Jennifer L. Murphy, Donna M. Muzny, Michele E. Nehrebecky, Stan F. Nelson, J. Scott Newberry, John H. Newman, Sarah K. Nicholas, Donna Novacic, Jordan S. Orange, J. Carl Pallais, Christina G.S. Palmer, Jeanette C. Papp, Neil H. Parker, Loren D.M. Pena, John A. Phillips III, Jennifer E. Posey, John H. Postlethwait, Lorraine Potocki, Barbara N. Pusey, Chloe M. Reuter, Amy K. Robertson, Lance H. Rodan, Jill A. Rosenfeld, Jacinda B. Sampson, Susan L. Samson, Kelly Schoch, Molly C. Schroeder, Daryl A. Scott, Prashant Sharma, Vandana Shashi, Rebecca Signer, Edwin K. Silverman, Janet S. Sinsheimer, Kevin S. Smith, Rebecca C. Spillmann, Kimberly Splinter, Joan M. Stoler, Nicholas Stong, Jennifer A. Sullivan, David A. Sweetser, Cynthia J. Tifft, Camilo Toro, Alyssa A. Tran, Tiina K. Urv, Zaheer M. Valivullah, Eric Vilain, Tiphanie P. Vogel, Colleen E. Wahl, Nicole M. Walley, Chris A. Walsh, Patricia A. Ward, Katrina M. Waters, Monte Westerfield, Anastasia L. Wise, Lynne A. Wolfe, Elizabeth A. Worthey, Shinya Yamamoto, Yaping Yang, Guoyun Yu, Diane B. Zastrow, and Allison Zheng.

Acknowledgments

This work is funded by the Undiagnosed Diseases Network U01HG007672 to V.S. and D.B.G., U01HG007703 to S.F.N., and U54NS093793 to H.J.B., S.Y., and M.J.W. H.J.B. is also supported by R01GM067858 and R24OD022005, and S.Y. and M.F.W. by a Simons Foundation Functional Screen Award (368479). We would like to thank Alejandro Lomniczi (OHSU) for sharing the *IRF2BPL* cDNA and Hongling Pan for technical assistance. Research reported in this publication was supported by the National Institute of Neurological Disorders and Stroke (NINDS) under award number K08NS092898 and Jordan's Guardian Angels (to G.M.). Confocal microscopy at Baylor College of Medicine is supported in part by NIH grant U54HD083092 to the Intellectual and Developmental Disabilities Research Center (IDDRC) Neurovisualization Core. H.J.B. is an Investigator of the Howard Hughes Medical Institute. The content is solely the responsibility of the authors and does not necessarily represent the official views of the NIH. The funding sources had no role in the design or conduct of the study, collection, management, analysis and interpretation of the data, preparation, review, or approval of the manuscript, or decision to submit the manuscript for publication. The authors would like to thank the subjects and their families for their participation.

Declaration of Interests

The Department of Molecular and Human Genetics at Baylor College of Medicine receives revenue from clinical genetic testing conducted by Baylor Genetics. David Goldstein is a founder of and holds equity in Pairnomix and Praxis, serves as a consultant to AstraZeneca, and has research supported by Janssen, Gilead, Biogen, AstraZeneca, and UCB.

Received: May 15, 2018
Accepted: July 2, 2018
Published: July 26, 2018

Web Resources

ClinVar, https://www.ncbi.nlm.nih.gov/clinvar/
ExAC, http://exac.broadinstitute.org/
GenBank, https://www.ncbi.nlm.nih.gov/genbank/
GeneMatcher, http://www.genematcher.org/
gnomAD, http://gnomad.broadinstitute.org/
MARRVEL, http://www.marrvel.org/
OMIM, http://www.omim.org/
Undiagnosed Diseases Network, https://undiagnosed.hms.harvard.edu
UDN *IRF2BPL* page, https://undiagnosed.hms.harvard.edu/genes/irf2bpl/

References

1. Iossifov, I., O'Roak, B.J., Sanders, S.J., Ronemus, M., Krumm, N., Levy, D., Stessman, H.A., Witherspoon, K.T., Vives, L., Patterson, K.E., et al. (2014). The contribution of de novo coding mutations to autism spectrum disorder. Nature *515*, 216–221.
2. de Ligt, J., Willemsen, M.H., van Bon, B.W.M., Kleefstra, T., Yntema, H.G., Kroes, T., Vulto-van Silfhout, A.T., Koolen, D.A., de Vries, P., Gilissen, C., et al. (2012). Diagnostic exome sequencing in persons with severe intellectual disability. N. Engl. J. Med. *367*, 1921–1929.
3. Deciphering Developmental Disorders Study (2017). Prevalence and architecture of de novo mutations in developmental disorders. Nature *542*, 433–438.
4. Amir, R.E., Van den Veyver, I.B., Wan, M., Tran, C.Q., Francke, U., and Zoghbi, H.Y. (1999). Rett syndrome is caused by mutations in X-linked MECP2, encoding methyl-CpG-binding protein 2. Nat. Genet. *23*, 185–188.
5. Chen, L., Chen, K., Lavery, L.A., Baker, S.A., Shaw, C.A., Li, W., and Zoghbi, H.Y. (2015). MeCP2 binds to non-CG methylated DNA as neurons mature, influencing transcription and the timing of onset for Rett syndrome. Proc. Natl. Acad. Sci. USA *112*, 5509–5514.
6. Kohlschütter, A., and Schulz, A. (2016). CLN2 disease (classic late infantile neuronal ceroid lipofuscinosis). Pediatr. Endocrinol. Rev. *13* (*Suppl 1*), 682–688.
7. Rakheja, D., Narayan, S.B., and Bennett, M.J. (2007). Juvenile neuronal ceroid-lipofuscinosis (Batten disease): a brief review and update. Curr. Mol. Med. *7*, 603–608.

8. Engelen, M., Kemp, S., and Poll-The, B.-T. (2014). X-linked adrenoleukodystrophy: pathogenesis and treatment. Curr. Neurol. Neurosci. Rep. *14*, 486.
9. Berger, J., and Gärtner, J. (2006). X-linked adrenoleukodystrophy: clinical, biochemical and pathogenetic aspects. Biochim. Biophys. Acta *1763*, 1721–1732.
10. Contreras, M., Mosser, J., Mandel, J.L., Aubourg, P., and Singh, I. (1994). The protein coded by the X-adrenoleukodystrophy gene is a peroxisomal integral membrane protein. FEBS Lett. *344*, 211–215.
11. Edvardson, S., Nicolae, C.M., Agrawal, P.B., Mignot, C., Payne, K., Prasad, A.N., Prasad, C., Sadler, L., Nava, C., Mullen, T.E., et al. (2017). Heterozygous de novo UBTF gain-of-function variant is associated with neurodegeneration in childhood. Am. J. Hum. Genet. *101*, 267–273.
12. Toro, C., Hori, R.T., Malicdan, M.C.V., Tifft, C.J., Goldstein, A., Gahl, W.A., Adams, D.R., Harper, F., Wolfe, L.A., Xiao, J., et al.; C4RCD Research Group (2018). A recurrent de novo missense mutation in UBTF causes developmental neuroregression. Hum. Mol. Genet. *27*, 691–705.
13. Chao, H.-T., Davids, M., Burke, E., Pappas, J.G., Rosenfeld, J.A., McCarty, A.J., Davis, T., Wolfe, L., Toro, C., Tifft, C., et al.; Undiagnosed Diseases Network (2017). A syndromic neurodevelopmental disorder caused by de novo variants in EBF3. Am. J. Hum. Genet. *100*, 128–137.
14. Luo, X., Rosenfeld, J.A., Yamamoto, S., Harel, T., Zuo, Z., Hall, M., Wierenga, K.J., Pastore, M.T., Bartholomew, D., Delgado, M.R., et al.; Members of the UDN (2017). Clinically severe CACNA1A alleles affect synaptic function and neurodegeneration differentially. PLoS Genet. *13*, e1006905.
15. Lupski, J.R., Reid, J.G., Gonzaga-Jauregui, C., Rio Deiros, D., Chen, D.C.Y., Nazareth, L., Bainbridge, M., Dinh, H., Jing, C., Wheeler, D.A., et al. (2010). Whole-genome sequencing in a patient with Charcot-Marie-Tooth neuropathy. N. Engl. J. Med. *362*, 1181–1191.
16. Oláhová, M., Yoon, W.H., Thompson, K., Jangam, S., Fernandez, L., Davidson, J.M., Kyle, J.E., Grove, M.E., Fisk, D.G., Kohler, J.N., et al.; Undiagnosed Diseases Network (2018). Biallelic mutations in *ATP5F1D*, which encodes a subunit of ATP synthase, cause a metabolic disorder. Am. J. Hum. Genet. *102*, 494–504.
17. Schoch, K., Meng, L., Szelinger, S., Bearden, D.R., Stray-Pedersen, A., Busk, O.L., Stong, N., Liston, E., Cohn, R.D., Scaglia, F., et al.; UCLA Clinical Genomics Center; and Undiagnosed Diseases Network (2017). A recurrent de novo variant in NACC1 causes a syndrome characterized by infantile epilepsy, cataracts, and profound developmental delay. Am. J. Hum. Genet. *100*, 343–351.
18. Shashi, V., Pena, L.D.M., Kim, K., Burton, B., Hempel, M., Schoch, K., Walkiewicz, M., McLaughlin, H.M., Cho, M., Stong, N., et al.; Undiagnosed Diseases Network (2016). De novo truncating variants in ASXL2 are associated with a unique and recognizable clinical phenotype. Am. J. Hum. Genet. *99*, 991–999.
19. Yoon, W.H., Sandoval, H., Nagarkar-Jaiswal, S., Jaiswal, M., Yamamoto, S., Haelterman, N.A., Putluri, N., Putluri, V., Sreekumar, A., Tos, T., et al. (2017). Loss of Nardilysin, a mitochondrial co-chaperone for α-ketoglutarate dehydrogenase, promotes mTORC1 activation and neurodegeneration. Neuron *93*, 115–131.
20. Lek, M., Karczewski, K.J., Minikel, E.V., Samocha, K.E., Banks, E., Fennell, T., O'Donnell-Luria, A.H., Ware, J.S., Hill, A.J., Cummings, B.B., et al.; Exome Aggregation Consortium (2016). Analysis of protein-coding genetic variation in 60,706 humans. Nature *536*, 285–291.
21. Wangler, M.F., Yamamoto, S., Chao, H.-T., Posey, J.E., Westerfield, M., Postlethwait, J., Hieter, P., Boycott, K.M., Campeau, P.M., Bellen, H.J.; and Members of the Undiagnosed Diseases Network (UDN) (2017). Model Organisms Facilitate Rare Disease Diagnosis and Therapeutic Research. Genetics *207*, 9–27.
22. Liu, X., Wu, C., Li, C., and Boerwinkle, E. (2016). dbNSFP v3.0: A one-stop database of functional predictions and annotations for human nonsynonymous and splice-site SNVs. Hum. Mutat. *37*, 235–241.
23. Wang, J., Al-Ouran, R., Hu, Y., Kim, S.-Y., Wan, Y.-W., Wangler, M.F., Yamamoto, S., Chao, H.-T., Comjean, A., Mohr, S.E., et al.; UDN (2017). MARRVEL: Integration of human and model organism genetic resources to facilitate functional annotation of the human genome. Am. J. Hum. Genet. *100*, 843–853.
24. Sobreira, N., Schiettecatte, F., Valle, D., and Hamosh, A. (2015). GeneMatcher: a matching tool for connecting investigators with an interest in the same gene. Hum. Mutat. *36*, 928–930.
25. Gahl, W.A., Wise, A.L., and Ashley, E.A. (2015). The Undiagnosed Diseases Network of the National Institutes of Health: A National Extension. JAMA *314*, 1797–1798.
26. Ramoni, R.B., Mulvihill, J.J., Adams, D.R., Allard, P., Ashley, E.A., Bernstein, J.A., Gahl, W.A., Hamid, R., Loscalzo, J., McCray, A.T., et al.; Undiagnosed Diseases Network (2017). The Undiagnosed Diseases Network: Accelerating discovery about health and disease. Am. J. Hum. Genet. *100*, 185–192.
27. Rampazzo, A., Pivotto, F., Occhi, G., Tiso, N., Bortoluzzi, S., Rowen, L., Hood, L., Nava, A., and Danieli, G.A. (2000). Characterization of C14orf4, a novel intronless human gene containing a polyglutamine repeat, mapped to the ARVD1 critical region. Biochem. Biophys. Res. Commun. *278*, 766–774.
28. GTEx Consortium (2013). The Genotype-Tissue Expression (GTEx) project. Nat. Genet. *45*, 580–585.
29. Rogers, S., Wells, R., and Rechsteiner, M. (1986). Amino acid sequences common to rapidly degraded proteins: the PEST hypothesis. Science *234*, 364–368.
30. Heger, S., Mastronardi, C., Dissen, G.A., Lomniczi, A., Cabrera, R., Roth, C.L., Jung, H., Galimi, F., Sippell, W., and Ojeda, S.R. (2007). Enhanced at puberty 1 (EAP1) is a new transcriptional regulator of the female neuroendocrine reproductive axis. J. Clin. Invest. *117*, 2145–2154.
31. Matagne, V., Mastronardi, C., Shapiro, R.A., Dorsa, D.M., and Ojeda, S.R. (2009). Hypothalamic expression of Eap1 is not directly controlled by ovarian steroids. Endocrinology *150*, 1870–1878.
32. Higashimori, A., Dong, Y., Zhang, Y., Kang, W., Nakatsu, G., Ng, S.S.M., Arakawa, T., Sung, J.J.Y., Chan, F.K.L., and Yu, J. (2018). Forkhead Box F2 suppresses gastric cancer through a novel FOXF2-IRF2BPL-β-catenin signaling axis. Cancer Res. *78*, 1643–1656.
33. Köhler, S., Vasilevsky, N.A., Engelstad, M., Foster, E., McMurry, J., Aymé, S., Baynam, G., Bello, S.M., Boerkoel, C.F., Boycott, K.M., et al. (2017). The human phenotype ontology in 2017. Nucleic Acids Res. *45* (D1), D865–D876.
34. Zhu, X., Petrovski, S., Xie, P., Ruzzo, E.K., Lu, Y.-F., McSweeney, K.M., Ben-Zeev, B., Nissenkorn, A., Anikster, Y., Oz-Levi, D., et al. (2015). Whole-exome sequencing in undiagnosed

genetic diseases: interpreting 119 trios. Genet. Med. *17*, 774–781.
35. Rehm, H.L., Berg, J.S., Brooks, L.D., Bustamante, C.D., Evans, J.P., Landrum, M.J., Ledbetter, D.H., Maglott, D.R., Martin, C.L., Nussbaum, R.L., et al.; ClinGen (2015). ClinGen–the Clinical Genome Resource. N. Engl. J. Med. *372*, 2235–2242.
36. Pollard, K.S., Hubisz, M.J., Rosenbloom, K.R., and Siepel, A. (2010). Detection of nonneutral substitution rates on mammalian phylogenies. Genome Res. *20*, 110–121.
37. Venken, K.J.T., Schulze, K.L., Haelterman, N.A., Pan, H., He, Y., Evans-Holm, M., Carlson, J.W., Levis, R.W., Spradling, A.C., Hoskins, R.A., and Bellen, H.J. (2011). MiMIC: a highly versatile transposon insertion resource for engineering Drosophila melanogaster genes. Nat. Methods *8*, 737–743.
38. Nagarkar-Jaiswal, S., Lee, P.-T., Campbell, M.E., Chen, K., Anguiano-Zarate, S., Gutierrez, M.C., Busby, T., Lin, W.-W., He, Y., Schulze, K.L., et al. (2015). A library of MiMICs allows tagging of genes and reversible, spatial and temporal knockdown of proteins in Drosophila. eLife *4*, 2743.
39. Diao, F., Ironfield, H., Luan, H., Diao, F., Shropshire, W.C., Ewer, J., Marr, E., Potter, C.J., Landgraf, M., and White, B.H. (2015). Plug-and-play genetic access to drosophila cell types using exchangeable exon cassettes. Cell Rep. *10*, 1410–1421.
40. Lee, P.-T., Zirin, J., Kanca, O., Lin, W.-W., Schulze, K.L., Li-Kroeger, D., Tao, R., Devereaux, C., Hu, Y., Chung, V., et al. (2018). A gene-specific *T2A-GAL4* library for *Drosophila*. eLife *7*, e35574.
41. Gnerer, J.P., Venken, K.J.T., and Dierick, H.A. (2015). Gene-specific cell labeling using MiMIC transposons. Nucleic Acids Res. *43*, e56.
42. Venken, K.J.T., Popodi, E., Holtzman, S.L., Schulze, K.L., Park, S., Carlson, J.W., Hoskins, R.A., Bellen, H.J., and Kaufman, T.C. (2010). A molecularly defined duplication set for the X chromosome of Drosophila melanogaster. Genetics *186*, 1111–1125.
43. Bischof, J., Maeda, R.K., Hediger, M., Karch, F., and Basler, K. (2007). An optimized transgenesis system for Drosophila using germ-line-specific phiC31 integrases. Proc. Natl. Acad. Sci. USA *104*, 3312–3317.
44. Venken, K.J.T., He, Y., Hoskins, R.A., and Bellen, H.J. (2006). P[acman]: a BAC transgenic platform for targeted insertion of large DNA fragments in D. melanogaster. Science *314*, 1747–1751.
45. Venken, K.J.T., Carlson, J.W., Schulze, K.L., Pan, H., He, Y., Spokony, R., Wan, K.H., Koriabine, M., de Jong, P.J., White, K.P., et al. (2009). Versatile P[acman] BAC libraries for transgenesis studies in Drosophila melanogaster. Nat. Methods *6*, 431–434.
46. Burg, M.G., and Wu, C.-F. (2012). Mechanical and temperature stressor-induced seizure-and-paralysis behaviors in Drosophila bang-sensitive mutants. J. Neurogenet. *26*, 189–197.
47. Madabattula, S.T., Strautman, J.C., Bysice, A.M., O'Sullivan, J.A., Androschuk, A., Rosenfelt, C., Doucet, K., Rouleau, G., and Bolduc, F. (2015). Quantitative analysis of climbing defects in a Drosophila model of neurodegenerative disorders. J. Vis. Exp. (100), e52741.
48. Jaiswal, M., Haelterman, N.A., Sandoval, H., Xiong, B., Donti, T., Kalsotra, A., Yamamoto, S., Cooper, T.A., Graham, B.H., and Bellen, H.J. (2015). Impaired mitochondrial energy production causes light-induced photoreceptor degeneration independent of oxidative stress. PLoS Biol. *13*, e1002197.
49. Duffy, J.B. (2002). GAL4 system in Drosophila: a fly geneticist's Swiss army knife. Genesis *34*, 1–15.
50. Petrovski, S., Wang, Q., Heinzen, E.L., Allen, A.S., and Goldstein, D.B. (2013). Genic intolerance to functional variation and the interpretation of personal genomes. PLoS Genet. *9*, e1003709.
51. Kircher, M., Witten, D.M., Jain, P., O'Roak, B.J., Cooper, G.M., and Shendure, J. (2014). A general framework for estimating the relative pathogenicity of human genetic variants. Nat. Genet. *46*, 310–315.
52. Jiang, Y., Han, Y., Petrovski, S., Owzar, K., Goldstein, D.B., and Allen, A.S. (2015). Incorporating functional information in tests of excess de novo mutational load. Am. J. Hum. Genet. *97*, 272–283.
53. Quinodoz, M., Royer-Bertrand, B., Cisarova, K., Di Gioia, S.A., Superti-Furga, A., and Rivolta, C. (2017). DOMINO: Using machine learning to predict genes associated with dominant disorders. Am. J. Hum. Genet. *101*, 623–629.
54. Harel, T., Yoon, W.H., Garone, C., Gu, S., Coban-Akdemir, Z., Eldomery, M.K., Posey, J.E., Jhangiani, S.N., Rosenfeld, J.A., Cho, M.T., et al.; Baylor-Hopkins Center for Mendelian Genomics; and University of Washington Center for Mendelian Genomics (2016). Recurrent de novo and biallelic variation of *ATAD3A*, encoding a mitochondrial membrane protein, results in distinct neurological syndromes. Am. J. Hum. Genet. *99*, 831–845.
55. Yamamoto, S., Jaiswal, M., Charng, W.-L., Gambin, T., Karaca, E., Mirzaa, G., Wiszniewski, W., Sandoval, H., Haelterman, N.A., Xiong, B., et al. (2014). A drosophila genetic resource of mutants to study mechanisms underlying human genetic diseases. Cell *159*, 200–214.
56. Tan, K.L., Haelterman, N.A., Kwartler, C.S., Regalado, E.S., Lee, P.-T., Nagarkar-Jaiswal, S., Guo, D.-C., Duraine, L., Wangler, M.F., Bamshad, M.J., et al.; University of Washington Center for Mendelian Genomics (2018). Ari-1 regulates myonuclear organization together with Parkin and is associated with aortic aneurysms. Dev. Cell *45*, 226–244.e8.
57. Liu, N., Schoch, K., Luo, X., Pena, L.D.M., Bhavana, V.H., Kukolich, M.K., Stringer, S., Powis, Z., Radtke, K., Mroske, C., et al.; Undiagnosed Diseases Network (UDN) (2018). Functional variants in TBX2 are associated with a syndromic cardiovascular and skeletal developmental disorder. Hum. Mol. Genet. *27*, 2454–2465.
58. Liaw, G.-J. (2016). Pits, a protein interacting with Ttk69 and Sin3A, has links to histone deacetylation. Sci. Rep. *6*, 33388.
59. Hu, Y., Flockhart, I., Vinayagam, A., Bergwitz, C., Berger, B., Perrimon, N., and Mohr, S.E. (2011). An integrative approach to ortholog prediction for disease-focused and other functional studies. BMC Bioinformatics *12*, 357.
60. Rohrbaugh, M., Clore, A., Davis, J., Johnson, S., Jones, B., Jones, K., Kim, J., Kithuka, B., Lunsford, K., Mitchell, J., et al. (2013). Identification and characterization of proteins involved in nuclear organization using Drosophila GFP protein trap lines. PLoS ONE *8*, e53091.
61. McGuire, S.E., Le, P.T., and Davis, R.L. (2001). The role of Drosophila mushroom body signaling in olfactory memory. Science *293*, 1330–1333.
62. Hsu, C.T., and Bhandawat, V. (2016). Organization of descending neurons in *Drosophila melanogaster*. Sci. Rep. *6*, 20259.
63. Dietzl, G., Chen, D., Schnorrer, F., Su, K.-C., Barinova, Y., Fellner, M., Gasser, B., Kinsey, K., Oppel, S., Scheiblauer, S., et al.

(2007). A genome-wide transgenic RNAi library for conditional gene inactivation in Drosophila. Nature *448*, 151–156.
64. Sumi-Akamaru, H., Beck, G., Kato, S., and Mochizuki, H. (2015). Neuroaxonal dystrophy in PLA2G6 knockout mice. Neuropathology *35*, 289–302.
65. Lin, G., Lee, P.T., Chen, K., Mao, D., Tan, K.L., Zuo, Z., Lin, W.W., Wang, L., and Bellen, H.J. (2018). Phospholipase PLA2G6, a Parkinsonism-Associated Gene, Affects Vps26 and Vps35, Retromer Function, and Ceramide Levels, Similar to α-Synuclein Gain. Cell Metab. https://doi.org/10.1016/j.cmet.2018.05.019.
66. Liu, L., Zhang, K., Sandoval, H., Yamamoto, S., Jaiswal, M., Sanz, E., Li, Z., Hui, J., Graham, B.H., Quintana, A., and Bellen, H.J. (2015). Glial lipid droplets and ROS induced by mitochondrial defects promote neurodegeneration. Cell *160*, 177–190.
67. Cusack, B.P., Arndt, P.F., Duret, L., and Roest Crollius, H. (2011). Preventing dangerous nonsense: selection for robustness to transcriptional error in human genes. PLoS Genet. *7*, e1002276.
68. Samocha, K.E., Robinson, E.B., Sanders, S.J., Stevens, C., Sabo, A., McGrath, L.M., Kosmicki, J.A., Rehnström, K., Mallick, S., Kirby, A., et al. (2014). A framework for the interpretation of de novo mutation in human disease. Nat. Genet. *46*, 944–950.
69. Firth, H.V., Richards, S.M., Bevan, A.P., Clayton, S., Corpas, M., Rajan, D., Van Vooren, S., Moreau, Y., Pettett, R.M., and Carter, N.P. (2009). DECIPHER: Database of Chromosomal Imbalance and Phenotype in Humans Using Ensembl Resources. Am. J. Hum. Genet. *84*, 524–533.
70. Marcogliese, P.C., Abuaish, S., Kabbach, G., Abdel-Messih, E., Seang, S., Li, G., Slack, R.S., Haque, M.E., Venderova, K., and Park, D.S. (2017). LRRK2(I2020T) functional genetic interactors that modify eye degeneration and dopaminergic cell loss in Drosophila. Hum. Mol. Genet. *26*, 1247–1257.
71. Chouhan, A.K., Guo, C., Hsieh, Y.-C., Ye, H., Senturk, M., Zuo, Z., Li, Y., Chatterjee, S., Botas, J., Jackson, G.R., et al. (2016). Uncoupling neuronal death and dysfunction in Drosophila models of neurodegenerative disease. Acta Neuropathol. Commun. *4*, 62.
72. Fergestad, T., Bostwick, B., and Ganetzky, B. (2006). Metabolic disruption in Drosophila bang-sensitive seizure mutants. Genetics *173*, 1357–1364.
73. Pavlidis, P., and Tanouye, M.A. (1995). Seizures and failures in the giant fiber pathway of Drosophila bang-sensitive paralytic mutants. J. Neurosci. *15*, 5810–5819.
74. Li, S., Wang, L., Berman, M., Kong, Y.-Y., and Dorf, M.E. (2011). Mapping a dynamic innate immunity protein interaction network regulating type I interferon production. Immunity *35*, 426–440.
75. Huttlin, E.L., Bruckner, R.J., Paulo, J.A., Cannon, J.R., Ting, L., Baltier, K., Colby, G., Gebreab, F., Gygi, M.P., Parzen, H., et al. (2017). Architecture of the human interactome defines protein communities and disease networks. Nature *545*, 505–509.
76. Xu, J., and Li, P. (2016). Expression of EAP1 and CUX1 in the hypothalamus of female rats and relationship with KISS1 and GnRH. Endocr. J. *63*, 681–690.
77. Li, C., and Li, P. (2017). Enhanced at puberty-1 (Eap1) expression critically regulates the onset of puberty independent of hypothalamic Kiss1 expression. Cell. Physiol. Biochem. *43*, 1402–1412.